

This is the peer reviewed version of the following article: “ Turim Koschevic, Marivane [et al.]. Antimicrobial activity of bleached cattail fibers (Typha domingensis) impregnated with silver nanoparticles and benzalkonium chloride. Journal of Applied Polymer Science. 2021; vol. 138, issue 35, 50885” which has been published in final form at <https://doi.org/10.1002/app.50885>. This article may be used for non-commercial purposes in accordance with [Wiley Terms and Conditions for Self-Archiving](#).”

1 **Antimicrobial activity of bleached cattail fibers (*Typha domingensis*)**
2 **impregnated with silver nanoparticles and benzalkonium chloride.**

3
4 Marivane Turim Koschevic¹; Renata Pires de Araújo¹; Vitor Augusto dos Santos Garcia²; Kelly
5 Mari Pires de Oliveira¹; Eduardo José Arruda¹; Alain Dufresne³; Sílvia Maria Martelli².

6
7 ¹PhD in Environmental Science and Technology. Faculty of Exact Sciences and Technology,
8 Federal University of Grande Dourados, Dourados, Brazil

9 ²Faculty of Engineering, Federal University of Grande Dourados, Dourados, Brazil

10 ³University Grenoble Alpes, Grenoble INP, LGP2, Grenoble, France

11
12 **Abstract:** Lignocellulosic fibers are renewable and sustainable materials, and their use
13 can be expanded when modified. This study aims to investigate the chemical
14 modifications in cattail fibers (*Typha domingensis* - *Taboa*) pretreated with alkaline
15 hydrogen peroxide (bleaching) and subsequently chemically modified by Tollens'
16 reagent for the deposition of silver nanoparticles (NP's) on the surface fibers and with
17 commercial quaternary ammonium salts (PolyCLBZ 50®, PolyQuat 08® and PolyBac
18 QT 80® from POLYORGANIC® Technology LTDA, São Paulo, Brazil), in order to
19 provide antimicrobial properties for these materials. After the treatments, they were
20 characterized by scanning electron microscopy, Fourier transform infrared
21 spectroscopy (FTIR), thermal properties (TGA/DTG) onset temperature (T_{onset}),
22 maximum degradation temperature (T_{max}) and residual mass, in addition to the profile
23 of antimicrobial susceptibility by means of disk-diffusion, against *Staphylococcus*
24 *aureus* (ATCC 25923), *Escherichia coli* (ATCC 25922), *Salmonella typhimurium*
25 (ATCC 14028) and *Salmonella enteritidis* (ATCC 13076). As a result, through SEM it
26 was possible to observe the silver nanoparticles on the surface of bleached fibers,
27 using FTIR, the presence of benzalkonium chloride was confirmed with the reduction
28 of the $3,400\text{ cm}^{-1}$ region, as well as by the presence of defined peaks in the region of
29 $2,921 - 2,851\text{ cm}^{-1}$ that can be attributed to characteristic stretches of alkanes binding
30 (CH bonds), and the increase in intensity by $1,383\text{ cm}^{-1}$, referring to tertiary amine. The
31 treatments applied influenced the thermal properties of the samples, with a small
32 reduction in stability when compared to the control fiber, as well as showing an
33 increase in residual mass. Regarding the susceptibility profile to microorganisms, it
34 was found that AgNP's are efficient for gram negative bacteria *E. coli*, *S. typhimurium*,

35 *S. enteritidis*. Samples with different concentrations of benzalkonium chloride showed
36 better activity against gram-positive bacteria *S. aureus*.

37

38 **Keywords:** Lignocellulosic fibers; Physical-chemical modifications; Immersion;
39 Impregnation; Tollens reagent; Benzalkonium chloride; Thermal properties;
40 Antimicrobial activity; Disc-Diffusion; Gram-Positive/Gram-Negative Bacteria.

41

42 1. Introduction

43

44 The use of cellulose is an area in constant expansion, not only for the production
45 of high-volume commodities, such as textiles and paper, but also for the discovery of
46 new materials with high added value, such as functionalized fibers and reinforcement
47 elements based on from natural fibers to composite materials (Belgacem & Gandini,
48 2005; Gandini & Belgacem, 2011), biocomposites and nanocomposites.

49 Considering the growing public health awareness about the pathogenic effects
50 caused by some microorganisms, there is a growing need to obtain antibacterial
51 materials, a strand with several areas of application, such as medical devices, hospital
52 materials, surgical equipment, hygiene applications household, textiles, food
53 packaging and storage (Goldade & Vinidiktova, 2017).

54 Cattail (*Typha domingensis*) is an infesting aquatic macrophyte, considered a
55 perennial and emerging herbaceous that belongs to the *Typhaceae* family (Apfelbaum,
56 1985) is a perennial herbaceous plant), which develops spontaneously throughout
57 tropical and subtropical America (Bajwa et al., 2015).

58 Silver is the best known of the various heavy metals' toxic to microorganisms
59 (Borsa, 2012). Silver nanoparticles have efficient antimicrobial properties compared to
60 other salts due to their extremely large surface area, which provides better contact with
61 microorganisms. It is assumed as a mechanism of action that the nanoparticles adhere
62 to the cell membrane and penetrate inside the bacteria. The bacterial membrane
63 contains proteins with sulfur and the silver nanoparticles interact with these proteins in
64 the cell, as well as with compounds containing phosphorus, such as DNA. When
65 AgNPs enter the bacterial cell, they form a low molecular weight region at the center
66 of the bacterium, in which the bacterium clumps together, protecting the DNA from
67 silver ions. Thus, they preferentially attack the respiratory chain, affecting cell division

68 and, ultimately, leading to death. Nanoparticles release silver ions in bacterial cells,
69 which still increase their bactericidal activity (Rai et al., 2009).

70 Quaternary ammonium salts are cationic surfactant compounds with long alkyl
71 groups, considered to be well-known disinfectants. These carry a positive charge on
72 the nitrogen atom (N⁺) in solution. The antimicrobial effect of these, in general, is due
73 to an electrostatic rupture of the cell wall after invasion by a lipophilic chain of specific
74 length. The agent is not consumed in the process; therefore, the antimicrobial activity
75 is continuous, if this bioactive material is adhered to the surface. It is considered
76 unlikely that microorganisms will become resistant to this type of attack, as this would
77 involve an important change in the structure of their cell wall (Borsa, 2012; Thomas et
78 al., 2009).

79 Surface modifications in natural fibers are widely studied and have shown
80 promising results in several fields of research. Cruz and Figueiro (2016) did a
81 bibliographic review on the changes in natural fibers (Cruz & Figueiro, 2016).
82 Examples include the study by Kulpinski et al., (2012), which obtained luminescent
83 cellulose fibers (Kulpinski et al., 2012). Xiao et al., (2017) developed an easy strategy
84 for the preparation of cellulose fibers functionalized with alkynes with click reactivity
85 (Xiao et al., 2017). Sabzalian; Alam; Van De Ven, (2014) investigated through the
86 application of chemical processes the transformation of hydrophilic cellulose fibers into
87 non-hygroscopic hydrophobic fibers (Sabzalian et al., 2014). Chauhan and Mohanty
88 (2015) studied an easy one-step hydrothermal method for coating titanium (TiO₂)
89 nanoparticles (diameter of about 40-250 nm) on the surface of cellulose fibers that
90 were used to prepare paper matrices and showed excellent activity photocatalytic for
91 degradation the methyl orange dye in the presence of ultraviolet light and also showed
92 promising antibacterial activity against *Escherichia coli* (Chauhan & Mohanty, 2015).
93 Li et al., (2015) prepared cellulose/silver nanocomposite fibers by immersing the
94 cellulose fibers in an aqueous solution of AgNO₃, to synthesize Ag nanoparticles *in*
95 *situ*, in this study the experiment antibacterial has proved to be excellent antibacterial
96 activity of cellulose nanocomposite fibers against *Staphylococcus aureus* (Li et al.,
97 2015). At the forefront, Lazić et al., 2020, developed silver nanoparticles coated with
98 dextran to improve the barrier and control the antimicrobial properties of nanocellulose
99 films used in food packaging (Lazić et al., 2020).

100 In this sense, to obtain versatile materials with antimicrobial activity, this study
101 investigated physical-chemical processes of incorporation of silver nanoparticles and

102 impregnation of commercial quaternary ammonium salts in bleached cellulose fibers.
103 These modifications of modifications appear as promising alternatives to obtain
104 sustainable materials.

105

106 **2. Material and methods**

107

108 *2.1 Raw material and chemicals*

109

110 Cattail fibers (*Typha dominguensis*) were obtained directly from farmers in
111 Dourados (Lat: 22 ° 13'18 " South, Lon: 54 ° 48'23 " West), Mato Grosso do Sul - Brazil,
112 in July 2016 The samples were dried in an oven at 50°C with air circulation for 24 hours
113 and crushed in a knife mill with mesh > 100 mesh and stored in plastic containers.

114 The reagents used in the chemical treatments (mercerization and bleaching)
115 such as Sodium Hydroxide (NaOH) and Hydrogen Peroxide (H₂O₂ 50%) were acquired
116 from Sigma Aldrich® and Dinâmica® in an analytical degree. Silver nitrate (AgNO₃),
117 ammonium nitrate (NH₄NO₃), analytical grade dextrose acquired from Merck Co® were
118 used to prepare the Tollens reagent.

119 The commercial quaternary ammonium compounds used were donated by the
120 company POLYORGANIC® Tecnologia LTDA (São Paulo, Brazil). Whose trade names
121 are: PolyCLBZ 50®, PolyBac QT 80® and PolyQuat 08®, both obtained from high
122 purity coconut oil fatty acids through reactions with benzyl chloride, following strict
123 specifications of the international pharmacopoeia. According to the manufacturer, the
124 PolyCLBZ 50® product has a 50% concentration of active ingredient, the rest
125 represented by solvent and water. The PolyBac QT 80® product has a molecular
126 weight of 353.90 g/mol, amine salt 1.0% maximum and 80% concentration of active
127 ingredient. The PolyQuat 08® product is a solution containing dodecyl dimethyl benzyl
128 ammonium chloride, solvent and water, 80% in concentration, which has a molecular
129 weight of 340.0g/mol, with a chain distribution (Typical) in 70% C12 and 30% C14
130 (PolyorganicTecnologiaLTDA, 2012, 2014a, 2014b).

131 For the disc-diffusion antimicrobial analysis, Brain hearth infusion broth (BHI)
132 Muller Hinton (MH) from Sigma Aldrich® (Bauer et al., 1966) was used.

133

134 *2.2 Alkali and alkaline/hydrogen peroxide treatment*

135

136 The mercerization and bleaching of natural fibers is an important process for the
137 purification of cellulosic material, as, among benefits, it increases the availability of
138 cellulose molecules for interaction with the active agents used.

139 The first treatment is carried out in an alkaline solution of sodium hydroxide
140 (NaOH) at 5% in the proportion 1:20 g.mL⁻¹ for 4 hours in the form of 190 rpm in a
141 shaker at room temperature. Subsequently, the fibers were washed in water until
142 neutral pH and dried in an oven with air circulation for 24 hours at 50 ° C (Negawo et
143 al., 2019; Vijay et al., 2019).

144 A further bleaching step was carried out in an alkaline/hydrogen peroxide solution
145 in the proportion of 1:20 g.mL⁻¹ of solution. This solution was prepared in a 1: 1 ratio
146 with 50% hydrogen peroxide and 5% sodium hydroxide at 50°C under continuous
147 preparation for 1 hour. Afterwards, the fibers were washed in water until neutral pH
148 and dried in an air circulation oven at 50 ° C for 24 hours. With the dry fiber, the third
149 and fourth stages were carried out containing only 1:1 oxidizing hydrogen peroxide and
150 distilled water under preparation at 50 ° C for 1 hour. After this process, the fibers were
151 washed with distilled water and again dried in an oven with air circulation at 50 ° C for
152 24 hours, then stored in plastic containers for later stages.

153

154 2.3 Tollens reagent

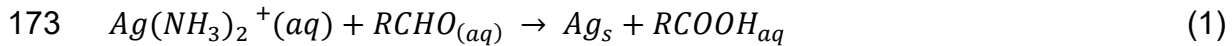
155

156 The Tollens reagent was prepared based on the methodology proposed by
157 Montarez, *et. al.*, (2012), and Michalcová *et al.*, (2018) with adaptations. First, silver
158 nitrate (0.5M) (AgNO₃), ammonium nitrate (1.5M) (NH₄NO₃), and dextrose (2M)
159 (C₆H₁₂O₆) solutions were prepared. Both prepared at room temperature and
160 atmospheric pressure. The ammonium nitrate solution (NH₄NO₃) was used as a
161 precursor, in which the second silver nitrate solution (AgNO₃) was added slowly until
162 the ratio 1:1 mL, with stirring (500rpm).

163 Initially, there was the formation of a brown precipitate, silver amine (complex ion
164 [Ag(NH₃)₂]⁺ + (Tollens' reagent), which disappeared after the complete mixing of the
165 solutions. Then 3mL of the dextrose solution was added, and the Tollens solution was
166 heated to 100°C. Afterward, 10g of bleached cattail fiber were added, which remained
167 in constant agitation (500rpm) at 100°C for 30 minutes. At the end of the process, the
168 fiber, initially white, showed a reddish-brown color. With the addition of dextrose
169 (aldehyde group) the Tollens reagent oxidizes the aldehyde group to a carboxylic acid

170 and, at the same time, induces the reduction of silver, in metallic silver, deposited on
171 the fibers. Process can be simplified in Equation 1.

172



174 Fonte: (Yin et al., 2002).

175

176 Subsequently, the fibers were washed with 500 mL of distilled water and dried in
177 an oven with air circulation at 50°C for 24 hours. After synthesis, the effluents
178 generated were acidified with dilute acid before disposal, to avoid the formation of
179 explosive silver nitride (Michalcová et al., 2018; Montazer et al., 2012).

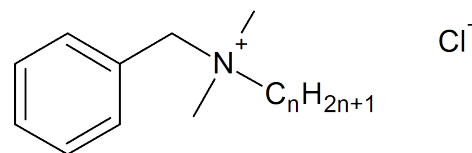
180

181 2.4 Quaternary ammonium salts solutions

182

183 The commercial quaternary solutions used had dodecyl dimethyl benzyl
184 ammonium chloride (benzalkonium chloride) – Fig. 1, solvent and water, with a
185 molecular weight of 340 g/mol. After the bleaching process, the dried fibers were
186 immersed in different solutions containing quaternary ammonium salts.

187



n = 8, 10, 12, 14, 16, 18

189 Fig. 1 Simplified typical chemical structure of benzalkonium chloride.

190 Source: (Álvarez-ros, 2018).

191

192 The solutions were prepared with the following concentrations of active
193 ingredient: 03.PolyCLBZ 50® [4%], 04.PolyQuat 08® [8%] and 05.PolyBac QT 80®
194 [10%], 06.PolyQT 08® [8 %]. In reagent glass flasks, solutions 03, 04 and 05 were
195 heated to 50°C, while solution 06 was heated to 85°C, after which bleached cattail
196 fibers [1g for each 50 mL] were added and the flasks were closed, 03, 04 and 05
197 remained immersed and under constant magnetic stirring (500 rpm) for 24 hours, while
198 solution 06 remained in the previous conditions for 6 hours (Adapted from He et al.,
199 2014; Wei et al., 2011). After the entire immersion process, the fibers were washed

200 with 500 mL of distilled water and dried in an oven for 24 hours at 50°C. Subsequently
201 stored in plastic containers for future analysis.

202

203 *2.5 Scanning electron microscopy (SEM)*

204

205 The microstructure and homogeneity of the modified fibers were observed using
206 SEM in a device called Quanta 200 FEI (Everhart - Thornley detector). Before
207 observation, samples were coated with gold. The sections were observed under an
208 acceleration voltage of 10 kV. Analysis performed at the LGP2 of the Polytechnic
209 Institute of Grenoble-France.

210

211 *2.6 Fourier transform infrared spectroscopy (FTIR)*

212

213 The analysis was performed using spectrophotometer model FT/IR-4100 type A
214 (JASCO®, Japan), transmission in KBr tablet. The spectra were recorded from 4000
215 to 500 cm^{-1} of wave numbers, with a resolution of 4 cm^{-1} and 32 scans, the analysis
216 was performed at the UFGD Optics Laboratory.

217

218 *2.7 Thermal properties*

219

220 Fiber samples of approximately 4 mg were placed in the platinum sample port
221 and subjected to a temperature range of 30 to 600°C at a heating rate (β) of 10°C.min⁻¹
222 and nitrogen atmosphere with a flow of 20 ml/min. The equipment used was the
223 simultaneous thermal analyzer STA 449 F3 Jupiter® (STA449 F3, NETZSCH®,
224 Germany), an analysis was carried out at the UFGD Thermal Analysis Laboratory.
225 Mass loss (TG curve) and first derivative (DTG curve) were compared as a function of
226 time/temperature.

227

228 *2.8 Antimicrobial susceptibility test*

229

230 To analyze the antimicrobial activity of the fibers after the modification, the disk
231 diffusion test (BAUER et al., 1966) was used, in which the standard species of
232 pathogens such as *Staphylococcus aureus* (ATCC 25923), *Escherichia coli* (ATCC
233 25922) were tested, *Salmonella enteritidis* (ATCC 13076) and *Salmonella*

234 typhimurium (ATCC 14028). It is a test that produces a qualitative result, such as the
235 classification of organisms in resistant, intermediate, or susceptible (ANVISA, 2005;
236 Sader & Pignatari, 1994; Performance Standards for Antimicrobial Disk Susceptibility
237 Tests, 13th Edition, 2018).

238 The microorganisms were reactivated in BHI broth (Brain heart infusion) for
239 24h in an oven at 37°C, sown on Muller Hinton agar (MH), and incubated for another
240 24h at 37°C, to obtain pure cultures. The test is carried out by applying a bacterial
241 inoculum of approximately $1-2 \times 10^8$ CFU/mL to the surface of a large Mueller-Hinton
242 agar plate (150 mm in diameter), in which up to 12 discs can be placed on the surface
243 of the inoculated agar. Subsequently, the plates are incubated for 16–24 h at 35 ° C.
244 The results are obtained by forming growth inhibition zones around each of the disks
245 used and measured with millimeter precision. The diameter of the zone is related to
246 the susceptibility of the isolate and the diffusion rate of the active agent in the agar
247 (Jorgensen & Ferraro, 2009).

248

249 *2.9 Statistical analysis*

250

251 The Statistica® 7.0 (StatSoft) software was used to calculate variance analyzes
252 (ANOVA) applied Tukey's test to determine differences between fibers properties in
253 the 95% confidence interval. To measure the diameters of the AgNP's, the free
254 software ImageJ® was used.

255

256 **3. Results and discussion**

257

258 *3.1 Initial characteristics, morphology, and infrared spectroscopy with Fourier* 259 *transform (FTIR)*

260

261 To contextualize the initial characteristics, Table 1 presents some data referring
262 to cattail fiber, before and after the bleaching process, in which it is possible to observe
263 improvements in the physical-chemical properties, such as increased cellulose
264 content, luminosity, crystallinity, onset temperature, maximum degradation
265 temperature and reduction in waste.

266 These chemical modifications referring to the purification of the cellulosic
267 material (mercerization and bleaching), are necessary to increase the availability of

268 hydroxyls (-OH) for the interaction with the compounds impregnated during the
269 functionalization of the material (Gandini & Belgacem, 2011). Some literature records
270 also show increases in cellulose content, crystallinity after mercerization/bleaching
271 procedures, such as cotton fibers (Adel et al., 2016), rice straw (Johar et al., 2012) and
272 *Cocconia grandis* L. fibers (Senthamaraikannan & Kathiresan, 2018).

273 Table 2 presents a brief description of the fiber samples with a summary of their
274 process and the code used for their identification.

275 As shown in Table 2, samples 04. CB + PQuat08 [8%] and 06. CB + PQT [8%]
276 85°C have the same concentration of active principle, differing only in the method of
277 obtaining, since fiber 06 was obtained with heating to 85°C and 6 hours of immersion
278 under agitation. Silver and other metals (and their ions) can be linked to cellulosic fibers
279 by several methods (Borsa, 2012), as examples the use of silver salt incorporated in
280 dressings with hydro cellulosic fibers used for wound healing, which presented
281 promising results, in helping to eliminate pathogens and wound healing (Newman et
282 al., 2006), as well as obtaining cotton fabrics padded with colloidal silver nanometer
283 solution (Lee et al., 2003).

284 In the images obtained by SEM – Fig. 2, it is possible to observe the presence
285 of silver nanoparticles deposited on the surface of the cattail fibers - Figure 2-02. While
286 the samples treated with different concentrations of quaternary ammonium remained
287 with homogeneous structures similar to the control fiber - Figure 2-01.

288 Fig. 2 - 02 shows the spherical structure of the AgNP's, with the aid of the
289 ImageJ® software, it was possible to measure their size, whose average area
290 measures 204 ± 0.06 nm. Montazer et al. (2012), in his study on the direct synthesis
291 of silver nanoparticles by Tollens' reagent in cotton fabric observed the formation of
292 nanoparticles that measured an average of 88 nm (Montazer et al., 2012). Thus, the
293 variation in the size of the nanoparticles is related to the synthesis process, studies
294 indicate that smaller particles were formed in lower concentrations of ammonia (Pingali
295 et al., 2008; Sharma et al., 2009). The size of the nanoparticle is important, as it directly
296 influences antimicrobial activity.

297 The FTIR spectra for the different modified and unmodified samples are
298 contained in Fig.3. The widest peak around $3,400\text{ cm}^{-1}$ for samples 01. CBC, 02. CB +
299 AgNp's, 03. CB + PCLBZ [4%] and 06. CB + PQT [8%] 85°C - 6h is due to elongation
300 of the cellulose -OH groups (Amroune et al., 2015), in samples 03. CB + PCLBZ [4%],
301 04. CB + PQuat08 [8%] and 05. CB + PBacQT [10%], there was a narrowing in this

302 region indicating that new interactions arose from immersion in different concentrations
303 of quaternary ammonium salts. The sample 06.CB + PQT 85% [8%] has the shortest
304 reaction time, 6 hours, in comparison to the other samples, a fact that may justify
305 maintaining the presence of the enlarged region at $3,400\text{ cm}^{-1}$.

306 Comparing the spectra of the modified fibers with quaternary in relation to the
307 control fiber, the presence of the active principle (benzalkonium chloride) is observed,
308 which was confirmed through the greater definition of the two peaks present in the
309 region of $2,921 - 2,851\text{ cm}^{-1}$ that can be attributed to characteristic stretches of CH-
310 type alkanes (Carvalho et al., 2009; Le Troedec et al., 2008; Ventura-Cruz et al., 2020),
311 evident especially in samples 04. CB + PQuat08 [8%] and 05. CB + PBacQT [10%], in
312 addition to the reduction of the extended band around $3,400\text{ cm}^{-1}$. In the region of
313 $1,626\text{ cm}^{-1}$ there is a characteristic peak of cellulosic materials that can be attributed
314 to the C=C aromatic vibration (Mahltig et al., 2004). This peak was more intense in
315 samples 04. CB + PQuat08 [8%] and 05. CB + PBacQT [10%] treated with quaternary
316 ammonium.

317 Yue et al., (2019) in their study on the addition and controlled release of
318 benzylammonium chloride (BAC) in nano-clays, as well as in this experiment also
319 observed the appearance of two new bands in the range of $2,900-2,850\text{ cm}^{-1}$, after
320 the addition of BAC, which were also attributed to the symmetric and asymmetric C -
321 H₂ elongation vibration of the alkyl group in BAC (Yue et al., 2019)

322 In the region of wave number $1,383\text{ cm}^{-1}$, the signal amplification for samples
323 04. CB + PQuat08 [8%] and 05. CB + PBacQT [10%] can be attributed to the angular
324 deformation C—H of the methyl group (CH₃) , as well as, can be defined as a
325 characteristic region of tertiary amines, intensified due to modification with
326 benzalkonium chloride (Liu et al., 2013). The C-O-C vibration of cellulose can be
327 observed by the prominent peak in the $1,057\text{ cm}^{-1}$ band (Adel et al., 2016). At 664
328 cm^{-1} , it's possible to see peaks referring to C-OH outside the plane referring to the
329 cellulose molecule (Le Troedec et al., 2008).

330 There are many -OH groups and in the cellulose fiber, which can be used to
331 reduce Ag⁺ in Ag. After the fibers are immersed in the Tollens reagent, it is considered
332 that it has penetrated their micropores, being then reduced by the -OH groups of the
333 cellulose. at 100°C , and simultaneously the cellulose was oxidized, a similar fact was
334 observed in the study by Li et al., (2015).

335 For the 02.CB + AgNp's sample, no characteristic bands were identified in its
336 spectrum, only that it remained similar to the 01.CBC control fiber. Li et al., (2015)
337 attributed the similarity of the modified spectra with silver nanoparticles to the control
338 fiber, the low concentration of AgNO₃ that would have oxidized few cellulose molecules
339 was oxidized, maintaining largely the cellulose structure.

340 With the data obtained, it appears that both the silver nanoparticles and the
341 samples with different concentrations of commercial ammonium quaternary were
342 successfully impregnated.

343

344 *3.2 Thermal properties and evaluation of the antimicrobial activity of fibers*

345

346 The thermal properties of a material are important to help define parameters
347 such as its use limitation. Fig. 4 shows the thermogravimetric (TG) and derived
348 thermogravimetric (DTG) curves obtained for the modified and unmodified fiber
349 samples.

350 The data obtained through the thermogravimetric analysis are compiled in Table
351 3. Thus, it is observed that the control sample 01.CBC has the greatest thermal
352 stability, or 336°C in Tonset, followed by the sample with 02. CB + AgNp's with 326°C,
353 and subsequently the sample 03.CB + PCLBZ [4%] and 05. CB + PBacQT [10%] at
354 321°C, samples 04. CB + PQuat08 and 06. CB + PQT 85°C [8%] at 311°C and
355 respectively the concentrations of 8% of active ingredient. Observing the DTG curves
356 - Figure 4-B, it can be seen in the samples with quaternary, the formation of a first peak
357 around 219°C, with the following values of mass loss of about 5% for samples 02. CB
358 + AgNp's, 03.CB + PCLBZ and 06. CB + PQT, about 7.5% for sample 04. CB +
359 PQuat08 and about 10% for sample 05. CB + PBacQT. Another event can be noticed
360 in the region of 282°C, with a loss of mass of about 10% for sample 02. CB + AgNp's,
361 about 14% for sample 06. CB + PQT, approximately 17% for sample 03. CB + PCLBZ
362 e, 22% for sample 05. CB + PBacQT. These events are related to the degradation of
363 benzalkonium chloride in the samples.

364 The quaternary concentration influences the thermal stability of the samples, for
365 the item maximum temperature of degradation, methodological differences for
366 obtaining samples 04 are still considered. CB + PQuat08 [8%] and 06. CB + PQT 85°C
367 [8%] as the temperature and time of obtaining differ in the number of final residues
368 sampled, being 5.5% to 3.5%.

369 In quantitative terms, when we try to better understand the concentration of
370 active principles in the samples, we can, with the help of the residual mass, calculate
371 the percentages of non-decomposed and non-volatile inorganic materials present in
372 the samples of AgNP's and commercial benzalkonium chloride. Thus, in Table 3 the
373 last column is reserved for the concentration of inorganic solids, corrected in relation
374 to the control sample 01.CBC.

375 As an estimate, it can be said that the sample 02. CB + AgNp's, has a
376 concentration of 3% of AgNP's. As for samples with quaternary ammonium, the
377 number of insoluble solids at 558°C varies according to the concentration and process
378 of application applied. These values may be related to the purity of the reagents used,
379 since these are commercial compounds.

380 The susceptibility profile to microorganisms was traced using standardized
381 strains and using the disk-diffusion technique - Figure 5. In Table 4, it is possible to
382 verify the values of inhibition halos obtained for the different samples, as well as their
383 control with known antibiotics. For the disk-diffusion test, 6 mm diameter discs obtained
384 by mechanically compacting the fibers in a metallic mold were standardized.

385 Figure 5 shows the zones of inhibition of the fibers impregnated against
386 *Staphylococcus aureus* (ATCC 25923) (gram-positive bacteria), *Escherichia coli*
387 (ATCC 25922), *Salmonella typhimurium* (ATCC 14028) and *Salmonella enteritidis*
388 (ATCC 13076) (gram-negative bacteria) respectively.

389 Pure bleached cattail fibers and antibiotics such as Oxacillin (1mg) and
390 Amikacin (30µg) were tested as control samples, for bleached cattail samples, no zone
391 of inhibition appeared, which illustrated that the fibers in question had no antibacterial
392 activity. The positive controls showed inhibition halos of about 18.5 mm. The sample
393 02.CB + AgNp's, showed activity only against gram-negative microorganisms, *E.coli*,
394 *S. typhimurium*, *S. enteritidis*, with medium halos of 8mm, we consider the
395 microorganisms tested for this sample condition resistant. The sample 03.CB +
396 PCLBZ, showed inhibition halos for the samples of gram-positive and negative
397 microorganisms, with clear inhibition zone for *S. aureus* 15mm, considered
398 intermediate, *E.coli*, 7mm, and *S. typhimurium*, 8mm, considered resistant. Samples
399 04.CB + PQuat08, 05.CB + PBacQT and 06.CB + PQT 85°C, presented inhibition halos
400 against gram-positive and negative microorganisms, *S. aureus*, values close to 15 mm,
401 considered intermediate and *E. coli*, and *S. enteritidis*, averages of 8.5 mm considered
402 resistant.

403 Regarding the results, its possible consider that all the modified samples of this
404 study showed relevant and significant antibacterial activity.

405 In the study by Mahltig et al., (2004) silica materials embedded with layers of
406 silver, silver salts and biocidal salts of quaternary ammonium (cetyltrimethylammonium
407 bromide and octenidine) were obtained and it was found that the growth of fungi and
408 bacteria could be inhibited (Mahltig et al., 2004).

409 Li et al., (2015) cellulose fibers were treated with silver nanoparticles and tested
410 for antibacterial activity against strains of *Staphylococcus aureus* and *E. Coli*, the
411 diameter of the inhibition zone and the photos taken were measured. It was found that
412 with the increase in the content of silver nanoparticles and the size of the particles in
413 the composite fibers, the antibacterial capacity increased. However, the inhibition halo
414 obtained for *E.coli* (21.0 mm) was smaller than that obtained for *Staphylococcus*
415 *aureus* (28.5 mm) for others silver became antibacterial through the destruction of the
416 bacterial cell wall, considering that the cell wall of these two bacteria was quite
417 different. The cell wall of *Staphylococcus aureus* is thicker with less protein content
418 than the cell wall of *E. coli*, therefore, *Staphylococcus aureus* is more easily (Li et al.,
419 2015).

420 In this study, however, there was no halo of inhibition for *Staphylococcus*
421 *aureus*, among the justifications it is mentioned that the antimicrobial effects of silver
422 NPs depend on their size, shape and concentration (Rai et al., 2009).

423 Son et al., (2006) in his study on the transmission of durable antimicrobial
424 properties to cotton fabrics using quaternary ammonium salts, tested the antimicrobial
425 activity of the cotton sample treated against *Staphylococcus aureus* according to the
426 AATCC 100- 1999, and found that the treated tissue showed greater antimicrobial
427 activity compared to the untreated tissue (Son et al., 2006).

428 Pinto et al., (2009) in their study to obtain cellulose nanocomposites/Ag found
429 about the antibacterial activity carried out for *Bacillus subtilis*, *Staphylococcus aureus*
430 and *Klebsiella pneumoniae* that the silver nanoparticles present in cellulosic fibers in
431 concentrations as low as $5, 0 \times 10^{-4}\%$ by weight make these nanocomposites effective
432 antibacterial materials (Pinto et al., 2009).

433 Finally, Volova et al., (2018) describes the production of bacterial cellulose (BC)
434 composites with silver nanoparticles and antibiotics and compares their properties, the
435 disk diffusion method and the agitated flask culture method were used and showed
436 that all experimental composites had activity antibacterial pronounced against *E. coli*,

437 *Ps. eruginosa*, *K. pneumoniae* and *St. aureus*, and BC/antibiotic compounds were
438 more active than BC / AgNp; *S. aureus* was the most susceptible to the effect of BC
439 composites (Volova et al., 2018).

440

441 **4. Conclusions**

442

443 Bleached cattail fibers were modified by physical-chemical processes of
444 impregnation of silver nanoparticles using Tollens' reagent, and commercial
445 quaternary ammonium salts were successfully obtained. The nanoparticles were
446 adhered to the surface of the fibers, and had, on average, an area of 200 nm.
447 Modifications in FTIR and TGA/DTG were identified that confirm the impregnation of
448 benzalkonium chloride in different proportions in the samples. Regarding antimicrobial
449 activity, positive and satisfactory responses were obtained to control contamination by
450 everyday microorganisms. AgNP's are effective for gram negative bacteria *E. coli*, *S.*
451 *typhimurium*, *S. enteritidis*. Samples with different concentrations of benzalkonium
452 chloride showed better activity against gram-positive bacteria *S. aureus*. We anticipate
453 that the versatile use of these cellulosic materials can bring a promising strategy in
454 obtaining a wide range of materials with important antimicrobial activities.

455

456 **Acknowledgments**

457

458 The Brazilian institutions for research promotion: CAPES, CNPQ, FUNDECT.
459 CAPES/BR: Marivane Turim Koschevic/Sandwich Doctorate Program abroad - PDSE
460 - Notice no. 47/2017 - Selection 2018/Process Number: 8881.189683/2018-01.

461

462 **References**

- 463 Adel, A. M., El-Gendy, A. A., Diab, M. A., Abou-Zeid, R. E., El-Zawawy, W. K., &
464 Dufresne, A. (2016). Microfibrillated cellulose from agricultural residues. Part I:
465 Papermaking application. *Industrial Crops and Products*, 93, 161–174.
466 <https://doi.org/10.1016/j.indcrop.2016.04.043>
- 467 Álvarez-ros, M. C. (2018). *Vibrational study of benzalkonium chloride (1) interaction*
468 *with metallic ions and surfaces : surface enhanced Raman spectroscopy study of*
469 *(1) with human serum albumin*. 1(2), 14–19.
- 470 Amroune, S., Bezazi, A., Belaadi, A., Zhu, C., Scarpa, F., Rahatekar, S., & Imad, A.

471 (2015). Tensile mechanical properties and surface chemical sensitivity of technical
472 fibres from date palm fruit branches (*Phoenix dactylifera* L.). *Composites Part A:
473 Applied Science and Manufacturing*, 71, 95–106.
474 <https://doi.org/10.1016/j.compositesa.2014.12.011>

475 ANVISA. (2005). *Normas de Desempenho para Testes de Sensibilidade*
476 *Antimicrobiana*.

477 Apfelbaum, S. (1985). Cattail (*Typha* spp.) Management. *Natural Areas Journal*, 5.

478 Bajwa, D. S., Sitz, E. D., Bajwa, S. G., & Barnick, A. R. (2015). Evaluation of cattail
479 (*Typha* spp.) for manufacturing composite panels. *Industrial Crops and Products*,
480 75, 195–199. <https://doi.org/10.1016/J.INDCROP.2015.06.029>

481 Bauer, A. W., Kirby, W. M., Sherris, J. C., & Turck, M. (1966). Antibiotic susceptibility
482 testing by a standardized single disk method. *American Journal of Clinical
483 Pathology*, 45(4), 493–496. https://doi.org/10.1093/ajcp/45.4_ts.493

484 Belgacem, M. N., & Gandini, A. (2005). Surface modification of cellulose fibres.
485 *Polímeros*, 15(2), 114–121. <https://doi.org/10.1590/s0104-14282005000200010>

486 Borsa, J. (2012). Antimicrobial natural fibres. In *Handbook of Natural Fibres*.
487 Woodhead Publishing Limited. <https://doi.org/10.1533/9780857095510.2.428>

488 Carvalho, C. D., Bertagnolli, C., & Silva, M. G. C. (2009). Preparação e caracterização
489 de argilas organofílicas para adsorção de óleos. *XVII Congresso Interno de
490 Iniciação Científica Da Unicamp*.
491 <https://www.prp.unicamp.br/pibic/congressos/xviicongresso/paineis/070329.pdf>

492 Chauhan, I., & Mohanty, P. (2015). In situ decoration of TiO₂ nanoparticles on the
493 surface of cellulose fibers and study of their photocatalytic and antibacterial
494 activities. *Cellulose*, 22(1), 507–519. <https://doi.org/10.1007/s10570-014-0480-3>

495 Cruz, J., & Figueiro, R. (2016). Surface Modification of Natural Fibers: A Review.
496 *Procedia Engineering*, 155, 285–288.
497 <https://doi.org/10.1016/j.proeng.2016.08.030>

498 Gandini, A., & Belgacem, M. N. (2011). Modifying cellulose fiber surfaces in the
499 manufacture of natural fiber composites. In *Interface Engineering of Natural Fibre
500 Composites for Maximum Performance* (Issue i). Woodhead Publishing Limited.
501 <https://doi.org/10.1533/9780857092281.1.3>

502 Goldade, V. A., & Vinidiktova, N. S. (2017). Antimicrobial fibers. *Crazing Technology
503 for Polyester Fibers*, 51–80. <https://doi.org/10.1016/b978-0-08-101271-0.00003-6>

504 Johar, N., Ahmad, I., & Dufresne, A. (2012). Extraction, preparation and

505 characterization of cellulose fibres and nanocrystals from rice husk. *Industrial*
506 *Crops and Products*, 37(1), 93–99. <https://doi.org/10.1016/j.indcrop.2011.12.016>

507 Jorgensen, J. H., & Ferraro, M. J. (2009). Antimicrobial susceptibility testing: A review
508 of general principles and contemporary practices. In *Clinical Infectious Diseases*
509 (Vol. 49, Issue 11, pp. 1749–1755). Oxford Academic.
510 <https://doi.org/10.1086/647952>

511 Kulpinski, P., Erdman, A., Namyslak, M., & Fidelus, J. D. (2012). Cellulose fibers
512 modified by Eu 3+-doped yttria-stabilized zirconia nanoparticles. *Cellulose*, 19(4),
513 1259–1269. <https://doi.org/10.1007/s10570-012-9704-6>

514 Lazić, V., Vivod, V., Peršin, Z., Stoiljković, M., Ratnayake, I. S., Ahrenkiel, P. S.,
515 Nedeljković, J. M., & Kokol, V. (2020). Dextran-coated silver nanoparticles for
516 improved barrier and controlled antimicrobial properties of nanocellulose films
517 used in food packaging. *Food Packaging and Shelf Life*, 26, 100575.
518 <https://doi.org/10.1016/j.fpsl.2020.100575>

519 Le Troedec, M., Sedan, D., Peyratout, C., Bonnet, J. P., Smith, A., Guinebretiere, R.,
520 Gloaguen, V., & Krausz, P. (2008). Influence of various chemical treatments on
521 the composition and structure of hemp fibres. *Composites Part A: Applied Science*
522 *and Manufacturing*, 39(3), 514–522.
523 <https://doi.org/10.1016/j.compositesa.2007.12.001>

524 Lee, H. J., Yeo, S. Y., & Jeong, S. H. (2003). Antibacterial effect of nanosized silver
525 colloidal solution on textile fabrics. *Journal of Materials Science*, 38(10), 2199–
526 2204. <https://doi.org/10.1023/A:1023736416361>

527 Li, R., He, M., Li, T., & Zhang, L. (2015). Preparation and properties of cellulose/silver
528 nanocomposite fibers. *Carbohydrate Polymers*, 115, 269–275.
529 <https://doi.org/10.1016/j.carbpol.2014.08.046>

530 Liu, K., Lin, X., Chen, L., Huang, L., Cao, S., & Wang, H. (2013). Preparation of
531 microfibrillated cellulose/chitosan-benzalkonium chloride biocomposite for
532 enhancing antibacterium and strength of sodium alginate films. *Journal of*
533 *Agricultural and Food Chemistry*, 61(26), 6562–6567.
534 <https://doi.org/10.1021/jf4010065>

535 Mahltig, B., Fiedler, D., & Böttcher, H. (2004). Antimicrobial sol-gel coatings. *Journal*
536 *of Sol-Gel Science and Technology*, 32(1–3), 219–222.
537 <https://doi.org/10.1007/s10971-004-5791-7>

538 Michalcová, A., Machado, L., Marek, I., Martinec, M., Sluková, M., & Vojtěch, D. (2018).

539 Properties of Ag nanoparticles prepared by modified Tollens' process with the use
540 of different saccharide types. In *Journal of Physics and Chemistry of Solids* (Vol.
541 113). Elsevier Ltd. <https://doi.org/10.1016/j.jpcs.2017.10.011>

542 Montazer, M., Alimohammadi, F., Shamei, A., & Rahimi, M. K. (2012). In situ synthesis
543 of nano silver on cotton using Tollens' reagent. *Carbohydrate Polymers*, 87(2),
544 1706–1712. <https://doi.org/10.1016/j.carbpol.2011.09.079>

545 Negawo, T. A., Polat, Y., Buyuknalçaci, F. N., Kilic, A., Saba, N., & Jawaid, M. (2019).
546 Mechanical , morphological , structural and dynamic mechanical properties of
547 alkali treated Ensete stem fi bers reinforced unsaturated polyester composites.
548 *Composite Structures*, 207(June 2018), 589–597.
549 <https://doi.org/10.1016/j.compstruct.2018.09.043>

550 Newman, G. R., Walker, M., Hobot, J. A., & Bowler, P. G. (2006). Visualisation of
551 bacterial sequestration and bactericidal activity within hydrating Hydrofiber®
552 wound dressings. *Biomaterials*, 27(7), 1129–1139.
553 <https://doi.org/10.1016/j.biomaterials.2005.07.046>

554 Pingali, K. C., Deng, S., & Rockstraw, D. A. (2008). Effect of Ammonium Nitrate on
555 Nanoparticle Size Reduction. *Research Letters in Nanotechnology*, 2008, 1–4.
556 <https://doi.org/10.1155/2008/756843>

557 Pinto, R. J. B., Marques, P. A. A. P., Neto, C. P., Trindade, T., Daina, S., & Sadocco,
558 P. (2009). Antibacterial activity of nanocomposites of silver and bacterial or
559 vegetable cellulosic fibers. *Acta Biomaterialia*, 5(6), 2279–2289.
560 <https://doi.org/10.1016/j.actbio.2009.02.003>

561 PolyorgânicaTecnologiaLTDA. (2012). *POLYQUAT 08*.

562 PolyorgânicaTecnologiaLTDA. (2014a). *POLYBAC CLBZ 05*.

563 PolyorgânicaTecnologiaLTDA. (2014b). *POLYBAC QT 80*.

564 Rai, M., Yadav, A., & Gade, A. (2009). Silver nanoparticles as a new generation of
565 antimicrobials. *Biotechnology Advances*, 27(1), 76–83.
566 <https://doi.org/10.1016/j.biotechadv.2008.09.002>

567 Sabzalian, Z., Alam, M. N., & van de Ven, T. G. M. (2014). Hydrophobization and
568 characterization of internally crosslink-reinforced cellulose fibers. *Cellulose*, 21(3),
569 1381–1393. <https://doi.org/10.1007/s10570-014-0178-6>

570 Sader, H. S., & Pignatari, A. C. (1994). E test: a novel technique for antimicrobial
571 susceptibility testing. In *São Paulo medical journal = Revista paulista de medicina*
572 (Vol. 112, Issue 4, pp. 635–638). Associação Paulista de Medicina.

573 <https://doi.org/10.1590/s1516-31801994000400003>

574 Senthamaraikannan, P., & Kathiresan, M. (2018). Characterization of raw and alkali
575 treated new natural cellulosic fiber from *Coccinia grandis* . L. *Carbohydrate*
576 *Polymers*, 186(October 2017), 332–343.
577 <https://doi.org/10.1016/j.carbpol.2018.01.072>

578 Sharma, V. K., Yngard, R. A., & Lin, Y. (2009). Silver nanoparticles: Green synthesis
579 and their antimicrobial activities. *Advances in Colloid and Interface Science*,
580 145(1–2), 83–96. <https://doi.org/10.1016/j.cis.2008.09.002>

581 Son, Y. A., Kim, B. S., Ravikumar, K., & Lee, S. G. (2006). Imparting durable
582 antimicrobial properties to cotton fabrics using quaternary ammonium salts
583 through 4-aminobenzenesulfonic acid-chloro-triazine adduct. *European Polymer*
584 *Journal*, 42(11), 3059–3067. <https://doi.org/10.1016/j.eurpolymj.2006.07.013>

585 Thomas, M., Montenegro, D., Castaño, A., Friedman, L., Leb, J., Huang, M. L.,
586 Rothman, L., Lee, H., Capodiferro, C., Ambinder, D., Cere, E., Galante, J., Rizzo,
587 J. L., Melkonian, K., & Engel, R. (2009). Polycations. 17. Synthesis and properties
588 of polycationic derivatives of carbohydrates. *Carbohydrate Research*, 344(13),
589 1620–1627. <https://doi.org/10.1016/j.carres.2009.04.021>

590 Ventura-Cruz, S., Flores-Alamo, N., & Tecante, A. (2020). Preparation of
591 microcrystalline cellulose from residual Rose stems (*Rosa* spp.) by successive
592 delignification with alkaline hydrogen peroxide. *International Journal of Biological*
593 *Macromolecules*, 155, 324–329. <https://doi.org/10.1016/j.ijbiomac.2020.03.222>

594 Vijay, R., Lenin Singaravelu, D., Vinod, A., Sanjay, M. R., Siengchin, S., Jawaid, M.,
595 Khan, A., & Parameswaranpillai, J. (2019). Characterization of raw and alkali
596 treated new natural cellulosic fibers from *Tridax procumbens*. *International Journal*
597 *of Biological Macromolecules*, 125, 99–108.
598 <https://doi.org/10.1016/j.ijbiomac.2018.12.056>

599 Volova, T. G., Shumilova, A. A., Shidlovskiy, I. P., Nikolaeva, E. D., Sukovaty, A. G.,
600 Vasiliev, A. D., & Shishatskaya, E. I. (2018). Antibacterial properties of films of
601 cellulose composites with silver nanoparticles and antibiotics. *Polymer Testing*,
602 65, 54–68. <https://doi.org/10.1016/j.polymertesting.2017.10.023>

603 Performance Standards for Antimicrobial Disk Susceptibility Tests, 13th Edition,
604 National Committee for Clinical Laboratory Standards (NCCLS) (2018).
605 <https://clsi.org/standards/products/microbiology/documents/m02/>

606 Xiao, G., Ding, C., Song, F., Qian, X., & An, X. (2017). Facile strategy for preparation

607 of alkyne-functionalized cellulose fibers with click reactivity. *Cellulose*, 24(2), 591–
608 607. <https://doi.org/10.1007/s10570-016-1153-1>

609 Yin, Y., Li, Z. Y., Zhong, Z., Gates, B., Xia, Y., & Venkateswaran, S. (2002). Synthesis
610 and characterization of stable aqueous dispersions of silver nanoparticles through
611 the Tollens process. *Journal of Materials Chemistry*, 12(3), 522–527.
612 <https://doi.org/10.1039/b107469e>

613 Yue, X., Zhang, R., Li, H., Su, M., Jin, X., & Qin, D. (2019). Loading and sustained
614 release of benzyl ammonium chloride (BAC) in nano-clays. *Materials*, 12(22).
615 <https://doi.org/10.3390/ma12223780>

616